Pediatr Radiol (1994) 24: 29–32

Pediatric Radiology

Langerhans cell histiocytosis of bone: MR imaging

J. C. George, K. A. Buckwalter, M. D. Cohen, M. K. Edwards, R. R. Smith

Department of Radiology, James Whitcomb Riley Hospital for Children, Indiana University School of Medicine, Indianapolis, IN 46262, USA

Received: 9 August 1993/ Accepted: 22 October 1993

Abstract. Magnetic resonance (MR) images of 12 pathologically proven lesions of Langerhans cell histiocytosis (LCH) of bone were reviewed retrospectively. MR identified all lesions, three of which were not identified on plain radiographs. In all cases, MR showed greater abnormality than did plain radiographs. With one exception, all lesions were hypointense on T1-weighted images and hyperintense on T2-weighted images. The lesions and associated soft tissue abnormalities were very conspicuous on short TI inversion sequences and T1-weighted post-contrast images. Follow-up MR studies in two patients after chemotherapy showed decreased size and enhancement of lesions compared with baseline studies.

Langerhans cell histiocytosis (LCH), formerly "histiocytosis X", is a disease of children characterized by idiopathic proliferation of histiocytes in the reticuloendothelial system [1]. Clinically and radiographically, localized LCH of bone may simulate osteomyelitis, lymphoma, or Ewing sarcoma [2]. Nuclear medicine studies may be falsely negative [3]. CT scans are useful for defining the extent of cortical involvement and may show soft tissue involvement [1]. Prior reports of MR imaging in LCH describe its usefulness in demonstrating bone marrow and soft tissue involvement [2, 4]. In addition to describing our experience with routine and gadolinium-enhanced spin-echo technique, we report the appearance of LCH on short-TI inversion (STIR) sequences and following chemotherapy. We also show the usefulness of this imaging technique in symptomatic patients with negative radiographs and a clinical suspicion of bone involvement with LCH.

Patients and methods

The MR images of ten patients with a diagnosis of Langerhans cell histiocytosis were reviewed retrospectively. The patients ranged in age from 20 months to 17 years, with a mean age of 9 years. Nine of the ten patients were male. The primary complaint in all patients was bone pain, with the exception of one 20-month-old child with dissminated disease who was unable to move his hip. Two patients had follow-up MR studies after chemotherapy with vinblastine.

Eight patients had abnormal radiographs and two had normal radiographs. Six patients had CT scans, which were all abnormal. Six patients had bone scans, which were also all abnormal.

A diagnosis of Langerhans cell histiocytosis was made with core needle biopsy specimens of bone lesions in nine patients and liver biopsy in one patient. Computed tomography (CT) guidance was used in cases of vertebral body involvement. In all patients, the pathologic diagnosis was made by identification of Birbeck granules on electron microscopy or Langerhans cells on light microscopy in combination with positive S-100 and peanut lectin stains.

MR imaging examinations were conducted with superconducting MR units (Vista, Picker International, Highland Heights, Ohio; Signa, General Electric Medical Systems, Milwaukee, Wis.) operating at 1.5 T. One examination was performed on a 0.5-T (GE Signa) scanner. Spine, body and small surface coils were used depending on lesion location. Slice thickness and scan orientations were also varied with regard to lesion location. Conventional spin-echo pulse sequences were used in all patients to generate T1-weighted (TR/TE 400–800 ms/15–30 ms) and T2-weighted (TR/TE 1800–2050 ms/80–90 ms) images. Proton density images were obtained in six patients. STIR (TR/TE/TI 1800–3250 ms/30 ms/100–150 ms) sequences were obtained in four patients, two with vertebral lesions and two with long bone lesions. Five patients received intravenous gadolinium-DTPA (0.1 mmol/kg Magnevist, Berlex) followed by T1-weighted sequences. Two patients had baseline and post-chemotherapy scans consisting of routine spin-echo and T1-weighted post-contrast sequences.

Results

The findings are summarized in Table 1. Twelve lesions in ten patients were found. The locations included six in the vertebrae, two in the femur and one each in the pelvis, scapula, clavicle, and humerus. Eight patients had abnormal radiographs that showed lytic or permeative lesions. Two patients (nos. 1, 7) had normal radiographs. Six patients had CT scans, all of which were abnormal. In all cases, CT scans showed lytic lesions with varying degrees of cortical disruption. A definite soft tissue mass was identified in only one patient (no. 3) with a vertebral body lesion. Six

Correspondence to: J. C. George, University Hospital 0279, 550 North University Blvd., Indianapolis, IN 46202-5253, USA

Table 1. MR appearance of Langerhans cell histiocytosis of bone in ten patients

Patient no.	Lesion				MR						
	location	X-ray	CT	Bone scan	T1	T2	PD	Post-contrast T1	STIR	Soft tissue abnormality	
										CT	MR
1	Thoracic spine	Normal	Abnormal	Normal	Hypo	Hyper	Iso	Enhanced	NA	No	Yes
	Lumbar spine	Normal	Abnormal	Abnormal	Hypo	Hyper	Iso	Enhanced	NA	No	Yes
2	Lumbar spine	Abnormal	Abnormal	Abnormal	Hypo	Hyper	Hyper	Enhanced	NA	No	Yes
3	Lumbar spine	Abnormal	Abnormal	Abnormal	Hypo	Hyper	Hyper	Enhanced	Hyper	Yes	Yes
4	Thoracic spine	Abnormal	Abnormal	NA	Hypo	Hyper	Hyper	Enhanced	Hyper	No	Yes
	Iliac bone	Abnormal	Abnormal	NA	Hypo	Hyper	Iso	NA	NA	No	Yes
5	Femur	Abnormal	NA	NA	Hypo	Hyper	Iso	NA	Hyper	NA	Yes
6	Humerus	Abnormal	NA	Abnormal	Hypo	Hyper	Iso	NA	Hyper	NA	Yes
7	Femur	Normal	NA	Abnormal	Hyper	Hyper	NA	NA	NA	NA	Yes
8	Scapula	Abnormal	Abnormal	Abnormal	Hypo	Hyper	NA	NA	NA	No	Yes
9	Clavicle	Abnormal	Abnormal	NA	Hypo	Hyper	NA	NA	NA	No	Yes
10	Thoracic spine	Abnormal	NA	NA	Hypo	Hyper	NA	Enhanced	NA	NA	No

PD, Proton density; hypo, hypointense; hyper, hyperintense; iso, isointense; NA, not available

patients had bone scans, and all showed abnormal findings with focal areas of increased radionuclide uptake. In one patient (no. 1) with two lesions in the spine, only one lesion was identified by bone scans.

MR images were abnormal in all patients. In all cases, MR showed more extensive bone marrow and soft tissue abnormality than plain radiographs. MR images were abnormal in two patients (nos. 1, 7) with normal radiographs (Fig. 1). One patient had two vertebral body lesions and another patient had a lesion in the femur. In three patients (nos. 1, 2, 4) with spine lesions, T2-weighted and gadolinium-enhanced MR images showed soft tissue abnormality outside the vertebral body that was not appreciated on CT. MR also showed soft tissue abnormality in patients (nos. 4, 8, 9) with lesions involving the pelvis, scapula and clavicle that were not seen with CT. In three patients (nos. 5–7) with long bone lesions, MR showed greater bone marrow abnormality than plain radiographs (Fig. 2).

With one exception, lesions were mildly to moderately hypointense on T1-weighted images and hyperintense on T2-weighted images relative to muscle. One lesion in a 20-month-old child (7) was hyperintense on both T1- and T2-weighted images (Fig. 3). The lesions had a variable appearance on proton density images, ranging from isointense to hyperintense relative to muscle. After intravenous contrast, the lesions showed moderately intense enhancement. Soft tissue abnormality was identified as high signal intensity on T2-weighted and T1-weighted post-contrast images. In one patient (no. 1) with a vertebral lesion, paraspinal soft tissue abnormality was identified on post-contrast MR images only (Fig. 1). STIR sequences were done in four patients (nos. 3–6), and all lesions were identified with this technique. In two patients (nos. 5, 6) with long bone lesions, STIR showed very high signal intensity in the soft tissues adjacent to the involved bone (Fig. 3). The soft tissue abnormality was more conspicuous and more extensive than it was on T2-weighted images. In two patients (nos. 3, 4) with vertebral body lesions, STIR images showed high signal abnormality similar to that on T2-weighted images. Two patients were re-examined with MR within 6 months following chemotherapy and using similar protocols. The lesions were smaller and the signal intensity lower than in the baseline studies.

Discussion

The plain radiographic appearance of LCH depends on the site of involvement and stage of disease [1]. LCH of bone commonly affects the skull, where lesions are usually lytic with well-defined nonsclerotic margins [1]. However, the appearance is variable, and lesions in the early phase of the disease may appear aggressive with a permeative or "moth-eaten" pattern [1]. Periostitis may be present in the presence or absence of pathologic fracture [5]. In our series, we found expansile and nonexpansile lytic lesions most commonly. Two patients had permeative long bone lesions with benign-appearing periostitis. With one exception, patients with lesions involving the spine had compression deformities ranging from mild to severe "vertebra plana".

CT is helpful in determining the presence of cortical invasion, periostitis, and extraosseous soft tissue extension [5]. CT can also detect a sequestrum that may be seen in LCH, osteomyelitis and lymphoma [6]. In two patients with lesions of the scapula and clavicle, CT showed slight-

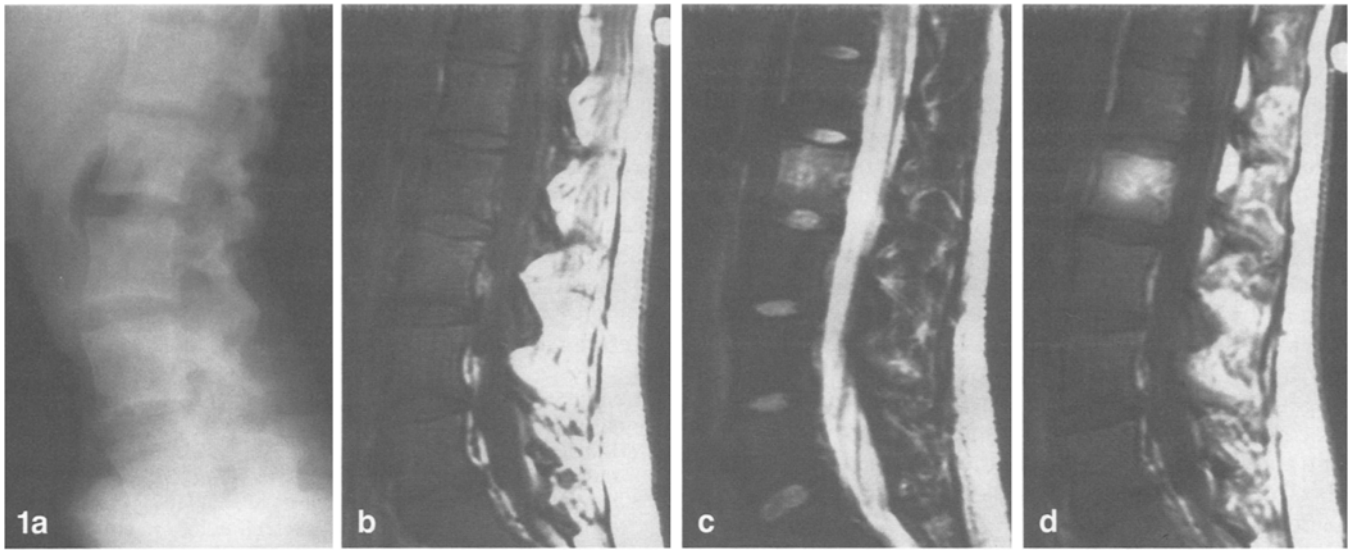

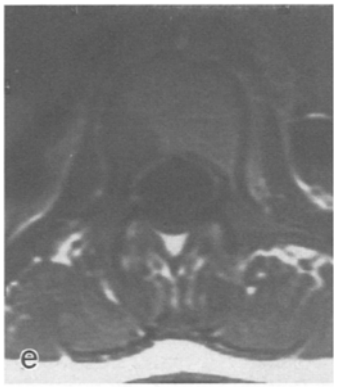

Fig. 1a–e. Sixteen-year-old girl with back pain.
a Normal radiograph.
b Sagittal T1-weighted MR image shows slightly hypointense lesion in L2 vertebral body.
c Sagittal T2-weighted MR image shows lesion is hyperintense.
d Sagittal T1-weighted post-contrast MR image shows lesion enhances.
e Axial T1-weighted post-contrast MR image shows soft tissue abnormality in left paravertebral region

Fig. 2a–c. Ten-year-old boy with leg pain.
a Radiograph shows lytic lesion in mid-shaft of left femur with subtle periostitis.
b T1-weighted coronal MR image shows more extensive marrow abnormality.
c Coronal STIR image shows juxtacortical soft tissue abnormality, probably representing reactive edema

Fig. 3. Twenty-month-old-child with Langerhans cell histiocytosis and immobile left hip. T1-weighted coronal MR shows hyperintense lesion in left femur replacing normal red bone marrow (compare with contralateral femur)

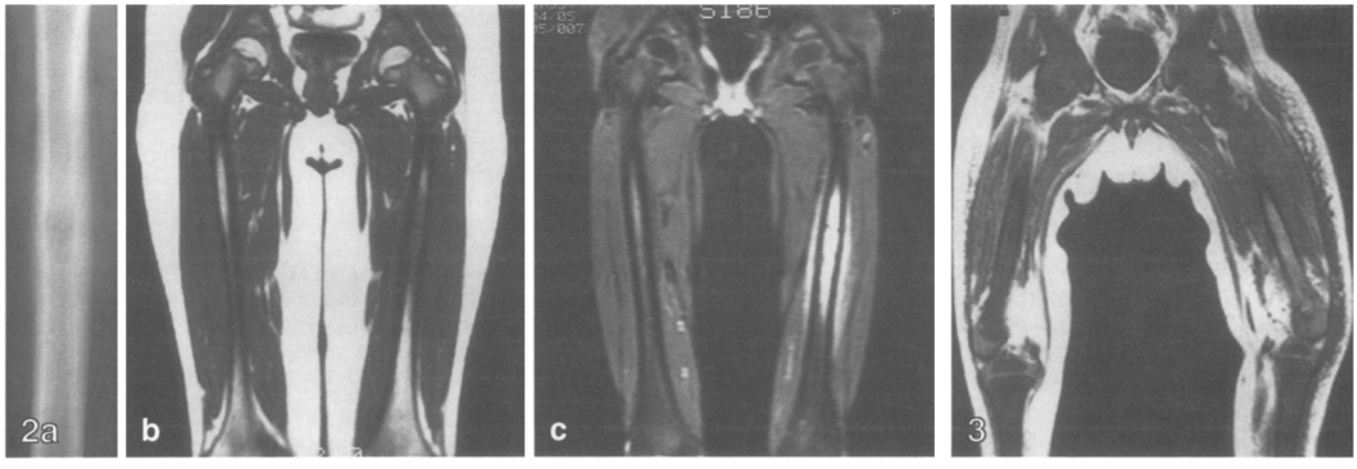

ly expansile lytic lesions with cortical disruption. Although definite soft tissue abnormality was seen on subsequent MR imaging, CT did not demonstrate this. In four patients with vertebral body lesions, CT showed lytic lesions with varying degrees of cortical destruction. Paraspinal soft tissue abnormality was identified in only one patient with certainty, although this finding was clearly seen on subsequent MR imaging in all cases. We suspect that this discrepancy may be due to the small size of the soft tissue component in these lesions.

Radionuclide bone scans most commonly show abnormal increased uptake in LCH lesions, but may be falsely negative [3]. With one exception, all lesions in our series showed abnormal increased uptake. The lesion that was not identified on bone scan was seen well on MR.

MR is useful in evaluation of disease processes affecting the bone marrow and soft tissue [7–10]. Because LCH involves both of these lcoations, MR is an effective imaging method. A number of processes, however, including benign and malignant tumors, infection, inflammation, and post-surgical changes, produce similar appearances on MR [11]. In cases of tumors of bone with a suspected soft tissue component, MR cannot reliably differentiate reactive edema from actual tumor invasion [9,

11]. This limitation of MR has been shown in MR-pathology studies of a number of benign and malignant lesions [12]. In cases of LCH, the prominent signal changes in adjacent bone marrow soft tissues have been attributed to inflammatory response, including reactive edema and increased free water [2].

Diseases that infiltrate bone marrow tend to decrease signal intensity on T1-weighted images due to replacement of marrow fat, which normally produces a bright T1 signal. The cellular marrow of children, however, has a longer T1 relaxation time than the fatty yellow marrow of adults [7]. The normal marrow in our 20-month-old child was hypointense relative to muscle on T1-weighted images. The affected marrow in this child was hyperintense on T1-weighted images compared with the normal contralateral side. This appearance suggests that the T1 relaxation time of the lesion was shorter than that of red marrow.

Due to its ability to nullify fat signal and to show the additive T1 and T2 contrast of pathologic processes, STIR imaging is useful in demonstrating bone marrow pathology [7, 13]. In our limited number of cases, STIR did not identify any lesions that were not shown on T2-weighted spin-echo or T1-weighted post-contrast sequences. It did, however, increase the conspicuousness of lesions and associated soft tissue abnormality compared with routine spin-echo sequences.

On follow-up MR scans of two patients with treated LCH lesions, T2-weighted and T1-weighted post-contrast MR scans showed decreased signal intensity and size compared with baseline studies. Because of our small sample size, we draw no conclusions. However, MR-pathology studies of some bone tumors have shown that a decrease in T2 signal intensity may reflect a good response to treatment [14, 15].

CT-guided biopsy is a common method of establishing the diagnosis of LCH involving the spine. As a result, axial MR images should be obtained. T1-weighed post-contrast images are an excellent way of demonstrating paraspinal soft tissue abnormality. T2-weighted and STIR images may be useful to avoid the expense of intravenous contrast. One must keep in mind, however, that MR is nonspecific and that biopsy of a soft tissue lesion may be negative due to reactive edema.

Our findings are in agreement with recent reports indicating that MR appears to be a sensitive imaging modality for identification of LCH involving bone. Our study indicates that MR scans may be abnormal in patients with symptoms of bone pain and normal radiographs. MR scans, including STIR images, may show soft tissue abnormality not evident with CT. Because it is nonspecific, the usefulness of MR in monitoring the results of nonsurgical therapy remains to be established.

References

1. Stull MA, Kransdorf MJ, Devaney KO (1992) Langerhans cell histiocytosis of bone. Radiographics 12: 801–823
2. Beltran J, Aparisi F, Bonmati LM et al (1993) Eosinophilic granuloma: MRI manifestations. Skeletal Radiol 22: 157–161
3. Siddiqui AR, Tashjian JH, Lazarus K et al (1981) Nuclear medicine studies in evaluation of skeletal lesions in children with histiocytosis X. Radiology 140: 787–789
4. De Schepper AMA, Ramon F, Van Marck E (1993) MR imaging of eosinophilic granuloma. Skeletal Radiol 22: 163–166
5. David R, Oria RA, Kumar R et al (1989) Radiologic features of eosinophilic granuloma of bone. AJR 153: 1021–1026
6. Mulligan ME, Kransdorf MJ (1993) Sequestra in primary lymphoma of bone: prevalence and radiologic features. AJR 160: 1245–1248
7. Vogler JB, Murphy WA (1988) Bone marrow imaging. Radiology 168: 679–693
8. Cohen MD, Klatte EC, Baehner RL et al (1984) Magnetic resonance imaging of bone marrow disease in children. Radiology 151: 715–718
9. Sundaram M, McLeod RA (1990) MR imaging of tumor and tumorlike lesions of bone and soft tissue. AJR 155: 817–824
10. Totty WG, Murphy WA, Lee JKT (1986) Soft tissue tumors: MR imaging. Radiology 160: 135–141
11. Beltran J, Simon DC, Katz W, Weis LD (1987) Increased MR signal intensity in skeletal muscle adjacent to malignant tumors: pathologic correlation and clinical relevance. Radiology 162: 251–255
12. Kransdorf MJ, Jelinek JS, Moser RP (1993) Imaging of soft tissue tumors. Radiol Clin North Am 31: 359–372
13. Dwyer AJ, Frank JA, Sank VJ et al (1988) Short-T1 inversion recovery pulse sequence: analysis and initial experience in cancer imaging. Radiology 186: 827–836
14. Vanel D, Lacombe M, Couanet D et al (1987) Musculoskeletal tumors: follow-up with MR imaging after treatment with surgery and radiation therapy. Radiology 164: 243–245
15. Holsher HC, Bloem JL, Nooy MA et al (1990) The value of MR imaging in monitoring the effect of chemotherapy on bone sarcomas. AJR 154: 763–769